Journal of Medicinal Chemistry

ARTICLE

pubs.acs.org/jmc

Radiosynthesis and Biological Evaluation of L- and D-*S*-(3-[^{18}F]Fluoropropyl)homocysteine for Tumor Imaging Using Positron Emission Tomography

Thomas Bourdier,*[,†] Rachael Shepherd,[†] Paula Berghofer,[†] Timothy Jackson,[†] Christopher J. R. Fookes,[†] Delphine Denoyer,[‡] Donna S. Dorow,[‡] Ivan Greguric,[†] Marie-Claude Gregoire,[†] Rodney J. Hicks,[‡] and Andrew Katsifis[†]

[†]ANSTO LifeSciences, Australian Nuclear Science and Technology Organisation, Locked Bag 2001, Kirrawee DC, NSW, 2232, Sydney, Australia

[‡]Centre for Molecular Imaging, The Peter MacCallum Cancer Centre, 12 St. Andrew's Place, East Melbourne, VIC, 3002, Australia

Supporting Information

ABSTRACT: Interest in radiolabeled amino acids for metabolic imaging of cancer and limitations with [^{11}C]methionine has prompted the development of a new ^{18}F-labeled methionine derivative *S*-(3-[^{18}F]fluoropropyl)homocysteine ([^{18}F]FPHCys). The L and D enantiomers of [^{18}F]FPHCys were prepared from their respective protected *S*-(3-tosyloxypropyl)homocysteine precursors **1** by [^{18}F]fluoride substitution using $K_{2.2.2}$ and potassium oxalate, followed by acid hydrolysis on a Tracerlab FX_{FN} synthesis module. [^{18}F]-L-FPHCys and [^{18}F]-D-FPHCys were isolated in 20 ± 5% radiochemical yield and >98% radiochemical and enantiomeric purity in 65 min. Competitive uptake studies in A375 and HT29 tumor cells suggest that L- and D-[^{18}F]FPHCys are taken up by the L-transporter system. [^{18}F]-L-FPHCys and [^{18}F]-D-FPHCys displayed good stability In Vivo without incorporation into protein at least 2 h postinjection. Biodistribution studies demonstrate good uptake in A375 tumor-bearing rodents with tumor to blood ratios of 3.5 and 5.0 for [^{18}F]-L-FPHCys and [^{18}F]-D-FPHCys, respectively, at 2 h postinjection.

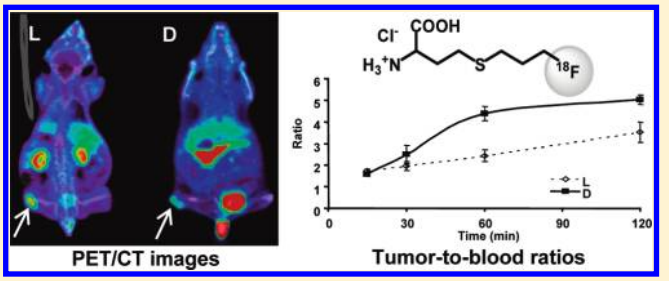

INTRODUCTION

Metabolic imaging employing positron emission tomography (PET) and [^{18}F]fluoro-2-deoxy-D-glucose ([^{18}F]FDG) has become firmly established as a routine clinical tool in tumor staging and for assessing tumor response to therapy. However, the high uptake of this tracer in the brain and nonmalignant, inflammatory tissue is a recognized limitation. New tracers are required, with greater sensitivity in areas of high physiological [^{18}F]FDG uptake and better specificity for tumor, particularly in situations, including surgery and irradiation, where inflammation is a part of the normal healing response or may be a complication of cancer or other diseases.[1]

It has long been recognized that amino acids play an important role in the growth of tumor cells,[2] providing an excellent opportunity for their use in clinical cancer imaging. Furthermore, the observation that amino acid imaging is less influenced by inflammatory processes suggests that they may overcome some of the disadvantages displayed by [^{18}F]FDG.[3] Several studies have already confirmed the clinical value of radiolabeled amino acids such as methionine (MET), fluoroethyl tyrosine (FET), and 2-fluorodopa (FDOPA) for imaging tumors in the brain.[4−6] There are less data relating to the utility of these agents in tumors outside the brain, but there are some encouraging reports in lymphoma,[7] lung,[8] and breast cancer.[9] Initial research and applications focused on carbon-11-labeled amino acids[10] and in particular *S*-(2-[^{11}C]methyl)-L-methionine ([^{11}C]MET), which has been extensively used in PET tumor imaging in both animals and man.[6]

However, the short half-life of carbon-11 has prompted the development of [^{18}F]-labeled amino acids ($t_{1/2}$ = 110 min) that are more convenient for routine PET applications.[11] Several [^{18}F]-labeled amino acids such as 2-[^{18}F]fluoro-L-tyrosine ([^{18}F]FT)[12−14] and 4-[^{18}F]fluoro-L-phenylalanine ([^{18}F]FPhe),[15] which are also incorporated into protein, have been evaluated and potentially allow the study of protein synthesis rates.[10,16] Although these amino acids have demonstrated encouraging imaging characteristics, their radiosynthesis is tedious and results in low radiochemical yield. Other [^{18}F]-labeled amino acids such as 2-[^{18}F]fluoro-α-methyl-L-tyrosine ([^{18}F]FMT),[17,18] *O*-(2-[^{18}F]-fluoroethyl)-L-tyrosine ([^{18}F]FET),[6,19−21] and [^{18}F]FDOPA are not incorporated into protein but have demonstrated value in studying amino acid transport processes in tumors.[20]

Received: November 24, 2010
Published: February 25, 2011

Scheme 1. Synthesis of Precursors 1−3[a]

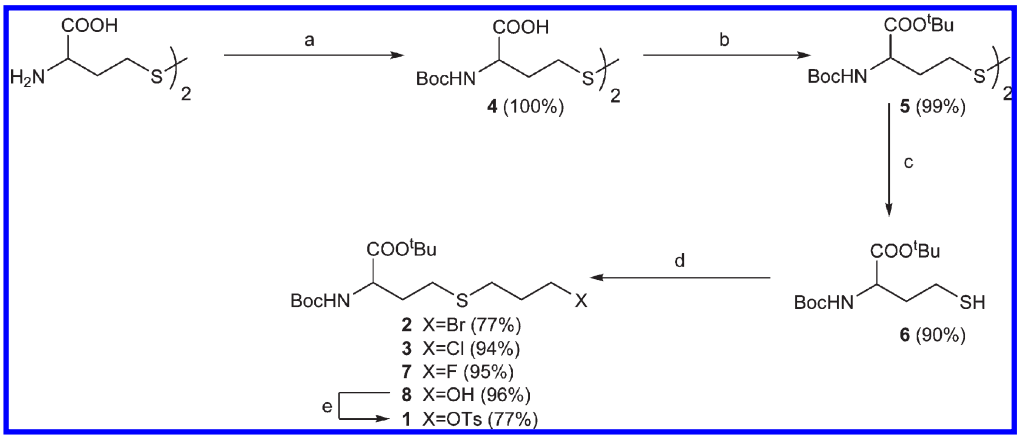

[a] Reagents and conditions: (a) Boc_2O, dioxane, $Na_2CO_{3(aq)}$, room temperature. (b) *tert*-Butyl-2,2,2-trichloroacetimidate, CH_2Cl_2, room temperature. (c) Tributylphosphine, DMF, room temperature. (d) 1-Bromo-3-halopropane or 3-bromopropanol, K_2CO_3, DMF, room temperature. (e) *p*-Toluenesulfonyl chloride, *N*,*N*,*N*′,*N*′-tetramethyl-1,6-hexanediamine, acetonitrile, room temperature.

Although some of these [^{18}F]-labeled amino acids have shown higher sensitivity in the evaluation of brain tumors than [^{18}F]FDG, their applications outside of the brain have generally been limited due to relative poor tumor uptake and substantial uptake in normal tissues, particularly skeletal muscle, yielding low to moderate tumor to background ratios. Recently, 2-amino-3-[^{18}F]fluoro-2-methylpropanoic acid ([^{18}F]FAMP),[22] 3-[^{18}F]fluoro-2-methyl-2-(methylamino)propanoic acid ([^{18}F]N-MeFAMP),[23] 1-amino-3-[^{18}F]fluorocyclobutyl-1-carboxylic acid ([^{18}F]FACBC),[24−26] and 1-amino-3-[^{18}F]fluoromethyl-cyclobutane-1-carboxylic acid ([^{18}F]FMACBC)[27] were synthesized with good tumor to brain ratios. Interestingly, the cyclobutyl amino acids have also shown promising results in imaging prostate tumors in man.

The convenient automated radiosynthesis of [^{11}C]MET via a [^{11}C]methyl thio-methylation and its role in amino acid transport and protein synthesis has made this amino acid one of the most frequently used in tumor imaging studies. However, its specificity and selectivity arre somewhat compromised due to the presence of competing biochemical reactions and the formation of a considerable amount of both protein and nonprotein radiolabeled metabolites. First, MET plays a very significant and competitive role in the activated methyl cycle, which serves as a methyl group donor in many biosynthetic steps through the formation of *S*-adenosylmethionine.[3,28] Consequently, a considerable amount of the carbon-11 activity coming from the [^{11}C]MET will contribute significantly to the background signal. Second, the incorporation of [^{11}C]MET into protein and the subsequent degradation of these products generate a considerable amount of radiolabeled metabolites.[29] Thus, the presence of both protein and nonprotein metabolites significantly contributes to a nonspecific signal, making quantitative imaging of amino acid transport and protein synthesis rates in tumors difficult.

Therefore, the development of an *S*-alkyl MET derivative that also incorporates a fluorine atom may first eliminate the competitive activated "methyl cycle" reactions by preventing the formation of *S*-adenosylmethionine and second reduce the capacity for incorporation into protein, thereby limiting the likelihood of metabolite production. Together, these effects could significantly reduce the nonspecific signal inherent in [^{11}C]MET imaging. In addition, further selectivity and specificity may be obtained by reducing the nonspecific signal by studying the D enantiomer of the fluoroalkyl derivatives. Finally, the incorporation of fluorine-18 onto a MET derivative would allow wider clinical applications due to the comparative longer half-life and wider distribution capability of this tracer to PET centers that are remote from a cyclotron.

Recently, a new amino acid analogue of MET, *S*-(2-[^{18}F]-fluoroethyl)-L-homocysteine ([^{18}F]FEHCys),[30,31] was synthesized. However, in our hands, [^{18}F]FEHCys was found to be unstable in aqueous systems, significantly limiting its use. For this reason, we have developed the D and L enantiomers of the fluoropropyl derivative *S*-(3-[^{18}F]fluoropropyl)homocysteine ([^{18}F]FPHCys). Here, we describe the preparation of [^{18}F]-L-FPHCys and [^{18}F]-D-FPHCys via a one-pot, two-step synthesis using the GE Tracerlab FX_{FN} synthesis module and report preliminary in vitro and In Vivo pharmacological evaluation.

RESULTS AND DISCUSSION

Chemistry. Our initial aim was to establish an efficient one-pot synthesis of [^{18}F]FPHCys using classical nucleophilic substitution reactions employing standard reagents and materials with retention of stereochemistry and suitable for routine clinical applications. Consequently, protected *S*-(3-tosyloxypropyl)homocysteine **1**, *S*-(3-bromopropyl)homocysteine **2**, and *S*-(3-chloropropyl)homocysteine **3** were synthesized as precursors and labeled with [^{18}F]fluoride. Although the tosyloxy derivative is generally the precursor of choice in [^{18}F]radiofluorination reactions, the corresponding brominated and chlorinated analogues were also prepared due to their ease of synthesis, stability, and good overall reactivity during radiolabeling and yield optimization. The synthesis of these precursors was achieved in four (**2** and **3**) or five steps (**1**) (Scheme 1).

Briefly, reaction of L-homocystine or D-homocystine with di-*tert*-butyl dicarbonate[32,33] gave the protected compound **4**, which upon reaction with *tert*-butyl-2,2,2-trichloroacetimidate[22,23,30] in dichloromethane at room temperature afforded quantitatively the disulfide **5**. Cleavage of the disulfide bond to form protected homocysteine **6** was achieved in 90% yield, using tributylphosphine in dimethylformamide (DMF).[30,33−35] Precursors **2** and

dx.doi.org/10.1021/jm101513q |*J. Med. Chem.* 2011, 54, 1860–1870

Scheme 2. Radiosynthesis of [^{18}F]FPHCys

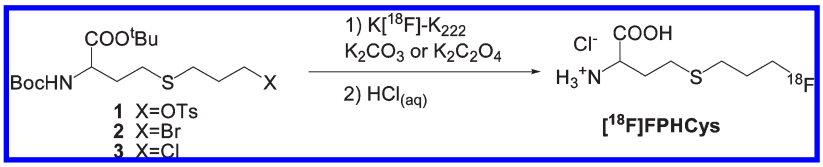

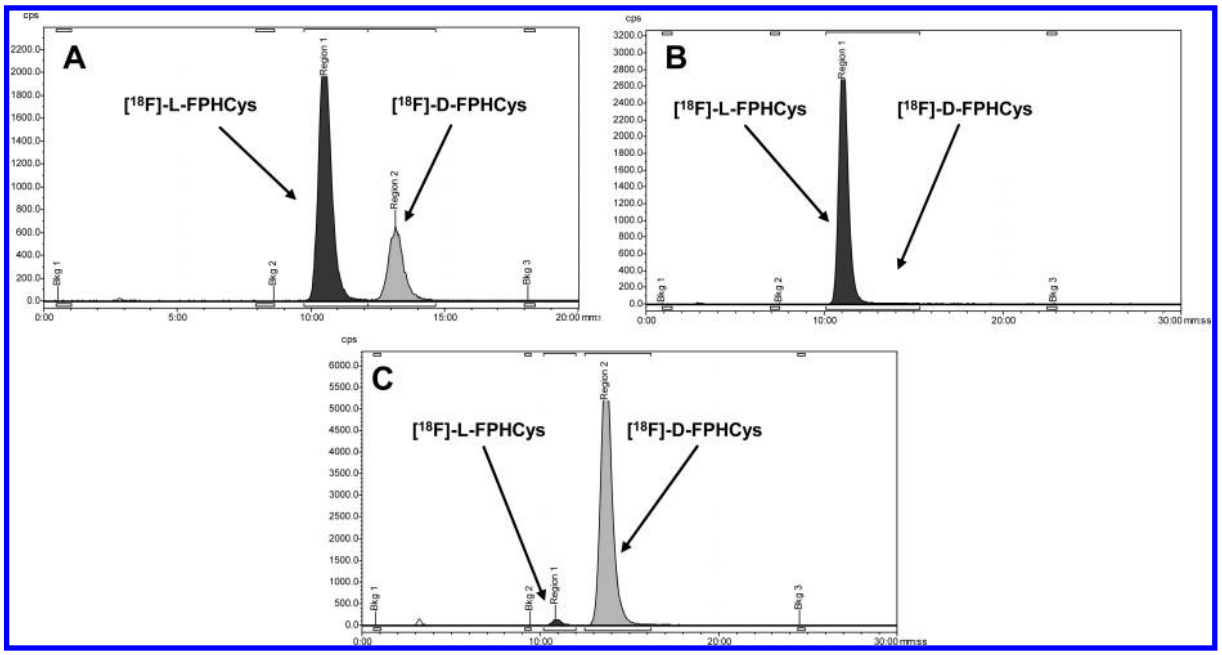

Figure 1. Radiochromatograms showing the enantiomeric purity of [^{18}F]-L-FPHCys using K_2CO_3 (A) or $K_2C_2O_4$ (B) and [^{18}F]-D-FPHCys using $K_2C_2O_4$ (C) during the radiolabeling. [^{18}F]-L-FPHCys and [^{18}F]-D-FPHCys have 10.5−11.5 and 13−14 min, respectively, as retention times.

3 and compounds **7** and **8** were prepared in 77−96% yields by coupling 1-bromo-3-halopropane or 3-bromopropanol with the thiol **6** in the presence of potassium carbonate in DMF at room temperature.[34,35] Protection of alcohol **8** with *p*-toluenesulfonyl chloride in the presence of *N,N,N′,N′*-tetramethyl-1,6-hexanediamine in acetonitrile was achieved in 77% yield.[36] The overall yields for the preparation of the tosyl-, bromo-, and chloro-precursors **1**−**3** were 65, 68, and 83%, respectively, for both the L and the D-enantiomers. Using this synthetic scheme, the enantiomeric purity of the final compounds as confirmed by chiral high-pressure liquid chromatography (HPLC) analysis was found to exceed 98%.

Radiochemistry. The initial radiosynthesis and yield optimization studies of [^{18}F]FPHCys involved the reaction of precursor **1** using classical [^{18}F]fluoride nucleophilic substitution[22,23,37] reactions in the presence of $K_{2.2.2.}$ and potassium carbonate, followed by acid hydrolysis of the protecting groups (Scheme 2). Briefly, the L-isomer of precursor **1** (10−14 μmol) was allowed to react with [^{18}F]fluoride in acetonitrile containing 10 mg of $K_{2.2.2.}$ and 2 mg of potassium carbonate at 100 °C for 15 min. Attempts to increase the radiochemical yield by extending the reaction time to 30 min led to a decreased yield of 73%, most likely due to decomposition. The intermediate [^{18}F]**7** was subsequently hydrolyzed with 6 N HCl at 100 °C for 5 min followed by neutralization with 6 N NaOH and dilution in phosphate buffer 1.5 M, pH 6. The resulting solution was purified by HPLC, but to increase the HPLC separation efficiency of [^{18}F]-L-FPHCys, evaporation of the acetonitrile posthydrolysis was required. Consequently, [^{18}F]-L-FPHCys was synthesized with an overall radiochemical yield of 30 ± 5% nondecay-corrected and a radiochemical purity >98%.

However, chiral HPLC analysis indicated that under these reaction conditions a partial racemization of the [^{18}F]-L-FPHCys had occurred, resulting in a final [^{18}F]-L-FPHCys/[^{18}F]-D-FPHCys ratio of 75:25 (Figure 1). Further analysis of both reaction steps indicated that racemization occurred during the initial radiolabeling step, brought about by proton abstraction of the α-hydrogen by the potassium carbonate base. Attempts to prevent or reduce racemization by varying the reaction conditions and precursor (**2** and **3**), for example, by decreasing reaction time and temperature (even down to 50 °C), were unsuccessful.

To avoid proton abstraction at the chiral center, one approach was to use either more hindered protecting groups or an alternative base. The use of *N*-trityl amino and *O*-*tert*-butyl ester protecting groups, as employed in the radiosynthesis of FET, successfully gave [^{18}F]FET in a moderate radiochemical yield with retention of chirality when potassium carbonate was employed as a base.[37,38] Another simpler approach was to use a weaker base with a pK_a < 10 (such as tetrabutylammonium hydrogencarbonate or potassium oxalate) for the labeling instead of potassium carbonate. In this study, potassium oxalate was

dx.doi.org/10.1021/jm101513q |*J. Med. Chem.* 2011, 54, 1860–1870

chosen because of the simplicity in reaction workup and purification. Thus, the radiolabeling of [^{18}F]-L-FPHCys was investigated with potassium oxalate (2.6 mg), $K_{2.2.2.}$ (10 mg), and precursors **1**−**3** (5 mg, 10−14 μmol) in acetonitrile at 50, 80, and 100 °C for 30 min. Under these conditions, the radiochemical yield obtained for the synthesis of the intermediate [^{18}F]**7** increased with temperature, with the highest at 100 °C for 30 min (62, 48, and 24% for precursors **1**, **2**, and **3**, respectively). In contrast to the use of potassium carbonate, potassium oxalate gave lower radiochemical yields for each precursor **1**−**3** investigated. Acid hydrolysis of the intermediate [^{18}F]**7** (generated from **1** for 10 min at 100 °C in 57% yield) with 6 N HCl at 100 °C for 5 min, followed by neutralization with 6 N NaOH, dilution with phosphate buffer 1.5 M, pH 6, and purification by HPLC produced [^{18}F]-L-FPHCys with a radiochemical purity of >98% and without racemization (Figure 1).

Finally, [^{18}F]-L-FPHCys was synthesized from precursor **1** by a one-pot, two-step synthesis, which has been fully automated on a GE Tracerlab FX_{FN} synthesis module in a reproducible nondecay-corrected radiochemical yield of 20 ± 5% and with a specific activity >185 GBq/μmol in approximately 65 min of preparation time including HPLC purification, formulation, and sterile filtration through a 0.22 μm filter for biological studies. The radiosynthesis of [^{18}F]-D-FPHCys from the precursor **1**−**3** (D-isomer) was accomplished using the same process as for the [^{18}F]-L-FPHCys and gave the same results with an enantiomeric purity >98% (Figure 1).

To investigate the biochemical properties of this new fluoropropyl MET derivative, cellular uptake studies, protein incorporation, metabolite, biodistribution, and imaging studies were performed for each enantiomer.

In Vitro Evaluation of [^{18}F]FPHCys. Cellular uptake studies of both [^{18}F]-L-FPHCys and [^{18}F]-D-FPHCys were conducted in A375 and HT29 tumor cell lines (Figure 2). In A375 cells, [^{18}F]-L-FPHCys rapidly accumulated with more than 50% of the total radioactivity accumulation occurring within the first 2 min of incubation. Uptake continued to increase for 60 min, reaching a maximum of 9% per 10^5 cells. Uptake of [^{18}F]-D-FPHCys was significantly lower than [^{18}F]-L-FPHCys at all time points. The uptake kinetics of [^{18}F]-D-FPHCys in A375 cells was rapid for the first 15 min and continued to increase at a slower rate from 15 to 60 min with the highest (6.8% per 10^5 cells) observed at 60 min. Cellular uptake in the HT29 cell line was significantly lower for both enantiomers with a maximum value of 2 and 1.6% per 10^5 cells for [^{18}F]-L-FPHCys and [^{18}F]-D-FPHCys, respectively, over 4 h.

To characterize the amino acid transport pathway used for [^{18}F]FPHCys uptake in tumor cells, competitive inhibition experiments were performed (Figure 3). Pretreating cells with 2-amino-bicyclo[2.2.1]heptane-2-carboxylic acid (BCH), an inhibitor of the amino acid transport system L, decreased the uptake of [^{18}F]-L-FPHCys by 98% in the A375 cell line and 86% in HT29 cells when compared to controls ($P < 0.05$). Uptake of [^{18}F]-D-FPHCys was decreased by 94 and 89% in A375 and HT29 cells, respectively ($P < 0.05$). In contrast, the A type amino acid transport inhibitor; *N*-methyl-α-aminoisobutyric acid (MeAIB) did not significantly block the uptake of [^{18}F]-L-FPHCys or [^{18}F]-D-FPHCys in either cell line. Therefore, cellular uptake of [^{18}F]-L-FPHCys and [^{18}F]-D-FPHCys in tumor cells was determined to be primarily via the amino acid transport system L. While uptake in A375 cells of [^{18}F]-L-FPHCys was higher than [^{18}F]-D-FPHCys, this uptake was not selective for the L-isomer over the D-isomer as the uptake of both isomers was blocked by BCH. This observation is consistent with that found for [^{11}C]MET.[39]

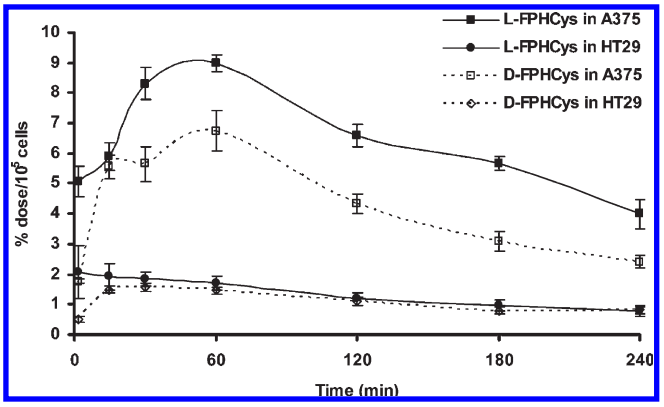

Figure 2. Cellular uptake of [^{18}F]-L-FPHCys and [^{18}F]-D-FPHCys in A375 and HT29 tumor cells. Data are means ± SDs (n = 3).

System L is responsible for transporting large neutral amino acids with branched or aromatic side chains such as leucine, isoleucine, valine, phenylalanine, tyrosine, tryptophan, histidine, and MET.[40] A subtype of this transport system, the L type amino acid transporter 1 (LAT1), has been reported to lack marked stereoselectivity.[40] The authors were able to demonstrate transport of ^{14}C-labeled D-leucine and D-phenylalanine by human LAT1 with high affinity and also showed that human LAT1-mediated transport of ^{14}C-leucine was inhibited by D-leucine, D-phenylalanine, and D-MET. Similarly, rat LAT2 transport of ^{14}C-leucine is also inhibited by D-isomers of serine, cysteine, and asparagines.[41] Therefore, the results from the in vitro cell uptake studies indicate that substitution of the *S*-methyl with an *S*-fluoropropyl moeity on MET did not affect its amino acid transport properties.

In Vivo Biodistribution of [^{18}F]FPHCys. The tissue distribution and kinetics of uptake for L- and D-enantiomers of [^{18}F]FPHCys in A375 tumor-bearing mice is summarized in Table 1. As expected, the % ID/g of [^{18}F]-L-FPHCys in all tissue (except the pancreas for the first hour) and blood was higher than that of [^{18}F]-D-FPHCys throughout the study. Consequently, the D-enantiomer exhibited a more rapid kidney extraction and clearance into the bladder. This observation was consistent with those reported for L- and D-[^{11}C]MET, *O*-^{11}C-methyl tyrosine, and *O*-^{18}F-fluoromethyl tyrosine.[44] The liver displayed a significantly higher uptake of [^{18}F]-L-FPHCys than the corresponding [^{18}F]-D-FPHCys with both displaying rapid clearance over the 2 h period studied. At 2 h, the uptake of the D-enantiomer in the liver was approximately one-third that of the L-enantiomer. Interestingly, the uptake of [^{18}F]-D-FPHCys in the pancreas was higher than the corresponding L-enantiomer for the first 30 min, but its clearance rate was faster than the L-enantiomer, resulting in a lower uptake from 1 h onward. Although the absolute uptake of [^{18}F]-L-FPHCys in the tumor was significantly higher than the D-enantiomer over the 2 h time period, the tumor-to-blood ratio of [^{18}F]-D-FPHCys was significantly higher than that of [^{18}F]-L-FPHCys (Figure 4). Both tracers showed longer retention in the tumor after 2 h as compared to the other organs in the periphery. Uptake of activity in the bone was lower for the D-enantiomer with both enantiomers displaying a steady decline. Although the bone/marrow composition was not analyzed individually, the declining activity over the 2 h period is not

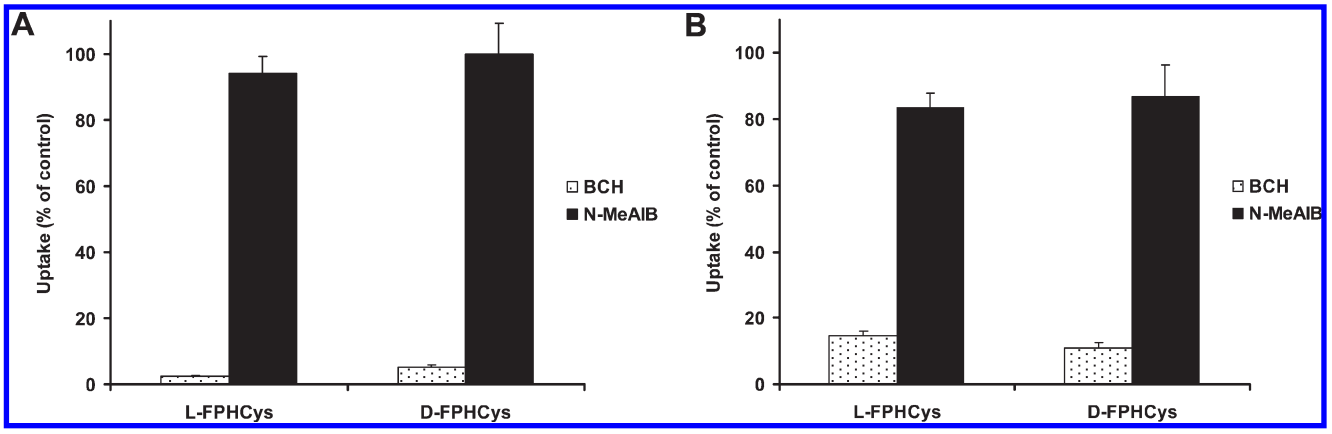

Figure 3. Blocking effect of specific amino acid transport inhibitors on [^{18}F]FPHCys uptake in A375 (A) and HT29 (B) cells. Data are means ± SDs (n = 3).

Table 1. Tissue Distribution of [^{18}F]-L-FPHCys and [^{18}F]-D-FPHCys in Balb/c Nude Mice Bearing A375 Tumors[a]

organ	isomer	15 min	30 min	60 min	120 min
liver	L	5.17 ± 0.74	4.84 ± 0.57	2.75 ± 0.43	1.92 ± 0.45
	D	3.96 ± 0.67	3.05 ± 0.38	1.49 ± 0.16	0.16 ± 0.69
spleen	L	5.05 ± 0.95	4.18 ± 0.64	2.11 ± 0.38	1.39 ± 0.31
	D	4.24 ± 0.79	2.83 ± 0.30	0.95 ± 0.14	0.31 ± 0.05
kidney	L	15.4 ± 1.20	12.6 ± 1.30	5.96 ± 0.61	3.92 ± 0.87
	D	12.2 ± 1.66	6.49 ± 1.20	2.75 ± 0.22	1.04 ± 0.28
muscle	L	4.12 ± 0.59	4.20 ± 0.37	2.52 ± 0.31	1.52 ± 0.37
	D	2.12 ± 0.40	1.97 ± 0.40	1.44 ± 0.05	0.63 ± 0.17
bone	L	3.33 ± 0.58	3.50 ± 0.57	2.31 ± 0.26	1.69 ± 0.29
	D	2.55 ± 0.41	2.29 ± 0.16	1.63 ± 0.10	1.05 ± 0.12
lungs	L	5.21 ± 0.32	5.07 ± 0.60	2.62 ± 0.33	1.63 ± 0.42
	D	4.11 ± 0.75	2.84 ± 0.75	1.55 ± 0.22	0.85 ± 0.13
heart	L	5.08 ± 0.36	4.20 ± 0.15	2.32 ± 0.46	1.37 ± 0.39
	D	3.92 ± 0.76	3.05 ± 0.40	1.16 ± 0.08	0.40 ± 0.16
brain	L	3.13 ± 0.58	2.57 ± 0.33	1.30 ± 0.25	2.57 ± 0.331
	D	1.53 ± 0.15	1.56 ± 0.29	0.75 ± 0.04	0.25 ± 0.03
pancreas	L	14.3 ± 2.66	12.3 ± 2.34	6.97 ± 1.18	3.77 ± 0.89
	D	37.1 ± 7.30	19.6 ± 3.97	4.79 ± 0.81	1.43 ± 0.25
blood	L	5.17 ± 0.80	4.44 ± 0.54	2.32 ± 0.33	1.38 ± 0.37
	D	3.51 ± 0.68	2.51 ± 0.35	0.89 ± 0.10	0.89 ± 0.100.3
tumor	L	9.41 ± 1.21	8.28 ± 0.81	5.64 ± 0.95	4.40 ± 0.67
	D	6.01 ± 0.77	5.87 ± 1.14	3.91 ± 0.32	1.68 ± 0.27

[a] Means ± SDs (n = 5). Data are expressed as % injected dose/g tissue.

indicative of any significant defluorination and subsequent bone fluoride uptake but most likely bone marrow uptake. This was further supported by PET/CT images, indicating uptake in bone regions with extensive marrow content (Figure 6).

Metabolite Studies. The stability and fate of [^{18}F]-L-FPHCys and [^{18}F]-D-FPHCys over time was analyzed in tumor, plasma, urine, pancreas, and brain (cortical) samples (Figure 5). The amount of unchanged tracer in tissue samples was determined by radio-HPLC.[42−44] After ultrasonic disruption of tissues in saline and centrifugation, at least 82% of the radioactivity in the tumor was recovered in the supernatant from samples collected at 0.25, 1, and 2 h for HPLC analysis. At least 85% of the radioactivity was recovered from the pancreas and brain from

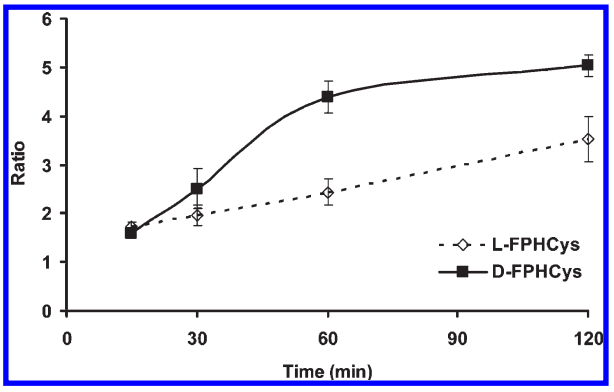

Figure 4. Time course of tumor-to-blood ratios of [^{18}F]-L-FPHCys and [^{18}F]-D-FPHCys in A375 tumor-bearing mice. The ratio of % ID/g of tumor against blood was determined for each time point in the biodistribution study.

samples collected at 0.25 and 1 h. The radioactivity collected from the 2 h samples was too low for detection by HPLC; therefore, metabolites were only analyzed up to 1 h in these tissues.

From the extracted activity, HPLC analysis indicated that more than 80% of the tracer remained intact after 2 h for both the L- and the D-enantiomers of [^{18}F]FPHCys in all tissues analyzed. In plasma, the percentage of unchanged [^{18}F]-L-FPHCys and [^{18}F]-D-FPHCys decreased from 90% at 0.25 h to 78% at 2 h postinjection. The composition of radioactive material extracted from the urine indicated that only 15% corresponded to intact [^{18}F]-L-FPHCys at 0.25 h postinjection, which was reduced to less than 4% at 2 h. In contrast, more than 75% of radioactivity in urine corresponded to intact [^{18}F]-D-FPHCys at 2 h postinjection. In the pancreas, more than 95% of the radioactivity represented [^{18}F]-D-FPHCys at 0.25 and 1 h. However, for the L-isomer, only 30% of radioactivity in the pancreas was intact tracer at 1 h. For both isomers, more than 90% of unchanged tracer was measured in the brain after 1 h.

A comparison of the metabolic stability of the two enantiomers of [^{18}F]FPHCys revealed that the D-isomer was more stable in all tissues studied, whereas the L-isomer was metabolized much faster as gauged by analysis of radioactive material in the urine and pancreas. Despite this, [^{18}F]-L-FPHCys was still remarkably stable in the plasma after 2 h. During the HPLC analysis, it was

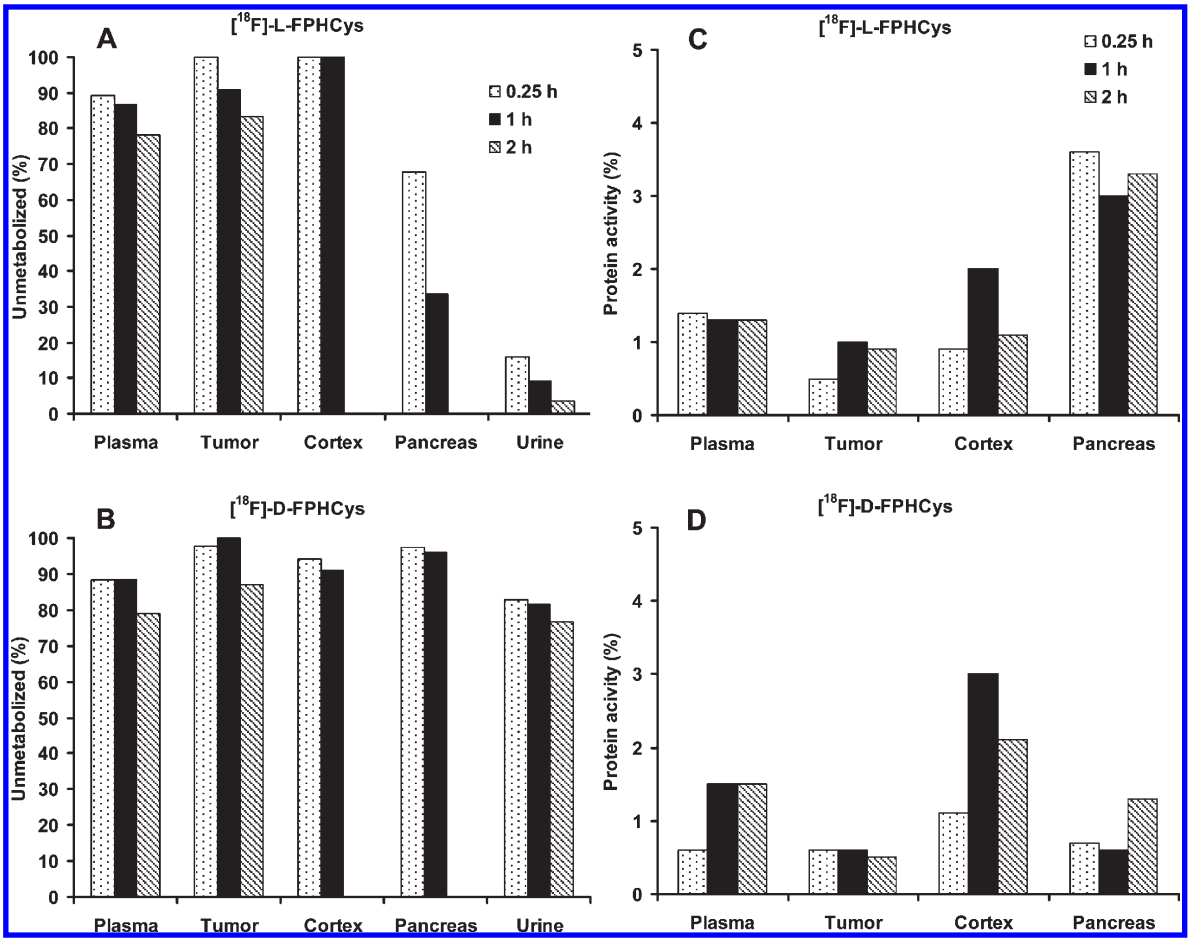

Figure 5. Percentage of unmetabolized [^{18}F]-L-FPHCys (A) and [^{18}F]-D-FPHCys (B) in plasma, tumor, brain (cortex), pancreas, and urine, as measured using radio-HPLC. The percentage incorporation of [^{18}F]-L-FPHCys (C) and [^{18}F]-D-FPHCys (D) into proteins in plasma, tumor, cortex, and pancreas, as measured using protein precipitation with trichloroacetic acid, was 0.25, 1, and 2 h after injection.

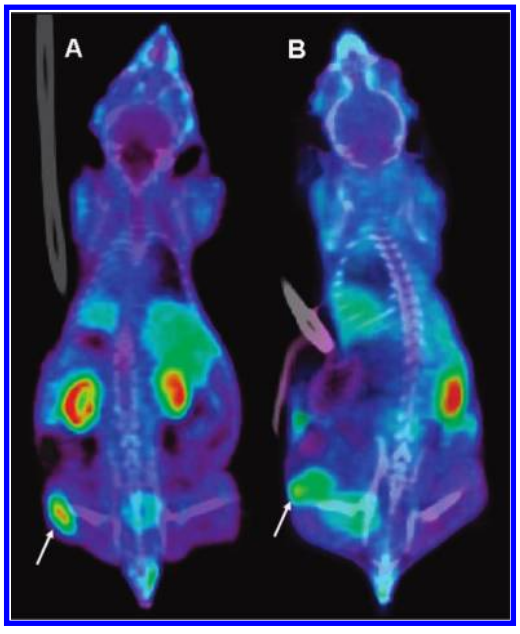

Figure 6. Coronal PET/CT images of Balb/c nude mice with A375 tumors (arrow) in the left flank at 60 min postinjection of [^{18}F]-L-FPHCys (A) and [^{18}F]-D-FPHCys (B).

shown that the main radioactive metabolites in tissues were highly polar products as they eluted with the solvent front. In a recent study, the stability of the L- and D-isomers of the unnatural amino acids, *O*-[^{11}C]methyl tyrosine ([^{11}C]CMT) and *O*-[^{18}F]-fluoromethyl tyrosine ([^{18}F]-FMT), was compared to the L- and D-isomer of [^{11}C]MET.[44] Metabolic analysis of the plasma demonstrated rapid metabolism of the natural amino acid [^{11}C]-L-MET, whereas the unnatural D-isomer remained unmetabolized up to 1 h. However, both isomers of the unnatural amino acids, [^{11}C]CMT and [^{18}F]FMT, also remained stable in the plasma. Finally, [^{18}F]-L-FPHCys and [^{18}F]-D-FPHCys were shown to be sufficiently stable In Vivo, 2 h after iv injection, to allow for their use as PET tracers of amino acid uptake in tumors.

Incorporation of [^{18}F]-L-FPHCys and [^{18}F]-D-FPHCys into Proteins. The extent of protein incorporation of [^{18}F]FPHCys was determined by protein precipitation with trichloroacetic acid (TCA)[42,43,45,46] (Figure 5) and size exclusion chromatography (SEC)[42] at 0.25, 1, and 2 h postinjection. Quantification of the incorporation of [^{18}F]-L-FPHCys and [^{18}F]-D-FPHCys into proteins by protein precipitation on aqueous extracts of tumor, frontal cortex, pancreas, and plasma homogenates resulted in only 1−4% of radioactivity present in the protein fractions (Figure 5). However, SEC of these samples showed no evidence of [^{18}F]-L-FPHCys and [^{18}F]-D-FPHCys incorporation into proteins even after 2 h due to the lower sensitivity of this

technique. Unlike [^{11}C]methyl-L-MET, which is actively incorporated into proteins, the structural modifications of the [^{18}F]-L-FPHCys and [^{18}F]-D-FPHCys indicated no incorporation.

PET Imaging Studies. The whole body distribution of [^{18}F]-L-FPHCys and [^{18}F]-D-FPHCys in A375 tumor-bearing mice (n = 3) was followed over 120 min using PET/CT imaging. Typical coronal PET images of both the [^{18}F]-L-FPHCys and the [^{18}F]-D-FPHCys administered into A375 tumor-bearing mice acquired at 60 min following radiotracer injection is shown in Figure 6.[47] In these images, the highest radioactivity concentration was observed in the kidneys, followed by the tumor. The radioactivity observed in the bladders of mice injected with [^{18}F]-D-FPHCys was higher than those injected with [^{18}F]-L-FPHCys. A lower background activity [^{18}F]-D-FPHCys in muscle and liver suggests potential advantages for clinical imaging. These observations confirmed the quantitative results obtained in the biodistribution studies. Interestingly, significant tracer uptake was observed in bone/marrow structures, confirming the biodistribution studies.

CONCLUSION

A new chemically stable, [^{18}F]-fluoropropyl derivative of MET was conveniently prepared from precursor **1** in a non-decay-corrected radiochemical yield of 20 ± 5%, in high radiochemical and enantiomeric purity and high specific activity for evaluation in tumor uptake studies. Unlike the fluoroethyl derivatives, [^{18}F]-L-FPHCys and [^{18}F]-D-FPHCys displayed good chemical stability for biological evaluation.

In Vivo studies of [^{18}F]-L-FPHCys and [^{18}F]-D-FPHCys in A375 tumor-bearing mice indicate a distribution profile not unlike that of [^{11}C]MET with high uptake in the tumor (9 and 6% ID/g at 15 min, respectively). Significantly, both the [^{18}F]-L-FPHCys and the [^{18}F]-D-FPHCys enantiomers displayed specific transport into tumor cells via the L-amino acid transporter. However, most importantly, the *S*-fluoropropyl fragment on MET inhibited the incorporation of both [^{18}F]-L-FPHCys and [^{18}F]-D-FPHCys into protein. It appears that the structural modifications made to MET via the introduction of the fluoroalkyl group renders this compound incompatible with the cell's protein synthesis machinery, yielding lower background signals for higher target to nontarget ratios. The fluoropropyl moiety of FPM may also avoid In Vivo *S*-methyl transfer biochemistry, potentially reducing side reactions and further reduce nonspecific signal. [^{18}F]-D-FPHCys, in particular, shows promising imaging characteristics with lower uptake and faster clearance of activity from normal tissues, resulting in a higher tumor to background ratio than for [^{18}F]-L-FPHCys.

EXPERIMENTAL SECTION

General. All reagents and solvents were purchased from Lancaster, Merck, or Sigma-Aldrich. All chemicals and solvents were used without further purification. *N*,*N*′-Di(*tert*-butoxycarbonyl)homocystine **4**, (*tert*-butyl) *N*,*N*′-bis(*tert*-butoxycarbonyl)homocystinate **5**, and *tert*-butyl *N*-(*tert*-butoxycarbonyl)homocysteinate **6** were prepared as described by Zhu et al. and Bourdier et al.[30,33] Sep-Pak Light QMA and Sep-Pak Light Alumina N were purchased from Waters. Millex GS 0.22 μm sterile filters were supplied from Millipore.

All melting points were determined in open capillary tubes using a SRS Optimet automated melting point system, MPA 100, and are uncorrected. ^{1}H and ^{13}C NMR spectra were measured on a Bruker DPX 400, at 400 MHz (^{1}H) and 100 MHz (^{13}C), in an appropriate deuterated solvent ($CDCl_3$, D_2O). Chemical shifts are reported as parts per million (δ) relative to tetramethylsilane (TMS, 0.00 ppm), which was used as an internal standard. Coupling constants are given in Hz, and coupling patterns are abbreviated as follows: s, singlet; d, doublet; t, triplet; q, quadruplet; qu, quintuplet; m, mutiplet; and dt, doublet of triplet. Low-resolution mass spectrometry (LRMS) was performed on a Waters Micromass ZQ Quadrupole Mass Spectrometer, whereas high-resolution mass spectrometry (HRMS) was performed using a Micromass Qtof Ultima or AutoSpec TOF. TLCs were run on precoated aluminum plates of silica gel $60F_{254}$ (Merck), and R_f values were established using an UV lamp at 254 nm or spraying with reagent. Column chromatography was undertaken on Merck 60 silica gel (40−63 μm) columns. The purity of all test compounds and key intermediates was determined to be >95% using an analytical HPLC, consisting of a Waters 600 gradient pump, a Waters 2489 UV detector (λ = 210 and 254 nm), and a Phenomenex Bondclone C18 column (300 mm × 7.8 mm, 10 μm). HPLC was run at 2 mL/min with acetonitrile (eluent I) and water (eluent II) and the following gradient: 1% acetonitrile for 3 min, ascending to 100% in 15 min and 100% for 10 min.

[^{18}F]HF was produced on a GE PET trace Cyclotron via the ^{18}O(p, n)^{18}F nuclear reaction (Cyclotek, Australia). The radiolabeling was performed on a GE Tracerlab FX_{FN} synthesis module (GE Medical Systems, Milwaukee, WI). The intermediate product labeled with fluorine-18 was analyzed by HPLC, consisting of a Waters 510 pump, a Linear UVIS detector (λ = 210 nm) in series with a Berthhold β^+-flow detector, on a Phenomenex Bondclone C18 column (300 mm × 7.8 mm, 10 μm) at 2 mL/min with CH_3CN/H_2O (75:25, v/v) as the mobile phase. *S*-(3-[^{18}F]fluoropropyl) homocysteine was purified by HPLC available on GE TracerLab FX_{FN} module, consisting of a Sykam S-1021 pump, a Knauer K-2001 UV detector (λ = 220 nm) in series with a Berthhold β^+-flow detector, on a Waters Atlantis C18 T3 column (250 mm × 10 mm, 5 μm) at 3 mL/min with ethanol/phosphate buffer, pH 6, 0.15 M (5:95, v/v) as the mobile phase. Quality control analysis of *S*-(3-[^{18}F]fluoropropyl) homocysteine was performed on a Varian 9002 pump and a Linear UV−vis detector (λ = 226 nm) in series with an Ortec ACE Mate β^+-flow detector on a Phenomenex Gemini column (150 mm × 4.6 mm, 5 μm) at 1 mL/min with phosphate buffer, pH 11.5, 0.05 M, as the mobile phase for chemical and radiochemical purity and on a Phenomenex Chirex D Penicillamine column (150 mm × 4.6 mm, 5 μm) at 1 mL/min with isopropanol/$CuSO_{4\ aq}$, 2 nM (1:9, v/v), as the mobile phase for enantiomeric purity. The identity of the labeled compound was confirmed by coinjection with the authentic compound on HPLC. The specific activity was determined by injection of an aliquot of the final solution with known volume and radioactivity on a Phenomenex Gemini analytical column (150 mm × 4.6 mm, 5 μm). The area of the UV absorbance peak measured at 226 nm corresponding to carrier product was measured and compared to a standard curve relating mass to UV absorbance. Only a specific activity below 185 GBq/μmol can be measure accurately due to the low absorbance of FPHCys in the UV. Radioactivity was measured with a Capintec R15C dose calibrator.

Metabolite studies were performed on a system consisting of a Waters 600 gradient pump, a Waters 486 UV detector (λ = 210 nm) in series with a β-Ram IN/US for measurement of radioactivity, and a Waters Atlantis C18 T3 column (150 mm × 4.6 mm, 5 μm) at 1 mL/min with methanol/phosphate buffer, pH 6, 0.15 M (5:95, v/v), as the mobile phase. The protein-bound activity was determined using a SEC on a system consisting of a Waters 600 gradient pump and a Waters 2489 UV detector (λ = 210 and 254 nm) in series with a Posi-Ram IN/US for measurement of radioactivity, on a Phenomenex BioSep SEC S2000 column (300 mm × 7.8 mm) at 1 mL/min with phosphate buffer, pH 7, 50 mM, as the mobile phase.

A375 human amelanotic melanoma cells and HT29 human colon adenocarcinoma cells were purchased from American Type Culture Collection. RPMI-1640 medium and L-glutamine were supplied from

Sigma-Aldrich, and 10% fetal bovine serum was purchased from Invitrogen.

All experimental procedures were performed in compliance with the NHMRC Australian Code of Practice for the care and use of animals for scientific purposes. Female Balb/c nude mice (5 weeks) were obtained from the Animal Resource Centre (WA, Australia). Mice were housed under constant environmental conditions and were allowed free access to food and water throughout the experimental period. In Vivo studies were performed in these mice bearing the A375 human amelanotic melanoma tumor. A375 cells were resuspended in Ca^{2+}- and Mg^{2+}-free PBS at 1×10^7 viable cells per mL of which 0.1 mL was injected subcutaneously in the left flank of 6 week old mice.

The mouse was anaesthetized via inhalant isoflurane (Forthane, Abbott) in 200 mL/min oxygen during the imaging study. PET imaging was performed on an Inveon multimodality PET/CT system (Siemens Medical Solutions, Knoxville, United States).

***tert*-Butyl *N*-(*tert*-butoxycarbonyl)-*S*-(3-fluoropropyl)-homocysteinate (7).** To a solution of 6 (445 mg, 1.53 mmol) in DMF (6.7 mL) was added 1-bromo-3-fluoropropane (326 mg, 2.29 mmol) followed by potassium carbonate (422 mg, 3.05 mmol), and the resultant white solution was stirred for 24 h at room temperature under nitrogen. The reaction mixture was diluted with water (90 mL) and extracted with ethyl acetate (3 × 45 mL). The combined organic layers were washed with water (90 mL) and dried ($MgSO_4$), and the solvents evaporated. The crude residue was purified by chromatography on silica gel (heptanes/ethyl acetate 90:10) to give **7** (504 mg, 95%) as a yellow oil. HPLC purity, 98%. ^{1}H NMR ($CDCl_3$, 400 MHz): δ 5.15−5.05 (m, 1H), 4.53 (dt, J = 47.1 Hz, J = 5.8 Hz, 2H), 4.35−4.20 (m, 1H), 2.64 (t, J = 7.3 Hz, 2H), 2.60−2.50 (m, 2H), 2.15−2.03 (m, 1H), 2.03−1.80 (m, 3H), 1.47 (s, 9H), 1.44 (s, 9H). ^{13}C NMR ($CDCl_3$, 100 MHz): δ 171.45, 155.48, 82.44 (J = 165.6 Hz), 82.35, 79.95, 53.55, 33.28, 30.54 (J = 20.7 Hz), 28.45, 28.15, 28.08, 27.90 (J = 5.4 Hz). LRMS: ES(+ve) m/z 374 (M + Na). HRMS: ES(+ve) calcd for $C_{16}H_{30}NO_4SF$ (M + 1), 352.1958; found, 352.1970.

***tert*-Butyl *N*-(*tert*-butoxycarbonyl)-*S*-(3-hydroxypropyl)-homocysteinate (8).** This compound was synthesized as described for **7** above, from **6** (6 g, 20.61 mmol) and 3-bromopropanol (4.43 mg, 30.92 mmol). The crude residue was purified by chromatography on silica gel (heptanes/ethyl acetate 70:30) to give **8** (6.91 mg, 96%) as a yellow oil. HPLC purity, 98%. ^{1}H NMR ($CDCl_3$, 400 MHz): δ 5.12−5.05 (m, 1H), 4.35−4.20 (m, 1H), 3.80−3.70 (m, 2H), 2.64 (t, J = 6.7 Hz, 2H), 2.60−2.50 (m, 2H), 2.15−2.05 (m, 1H), 1.95−1.80 (m, 2H), 1.83 (qu, J = 6.7 Hz, 2H), 1.47 (s, 9H), 1.44 (s, 9H). ^{13}C NMR ($CDCl_3$, 100 MHz): δ 172.56, 156.56, 82.35, 81.06, 61.62, 54.51, 33.18, 31.98, 28.80, 28.47, 28.16, 28.02. LRMS: ES(+ve) m/z 372 (M + Na). HRMS: ES(+ve) calcd for $C_{16}H_{31}NO_5S$ (M + 1), 350.2001; found, 350.2017.

***tert*-Butyl *S*-(3-bromopropyl)-*N*-(*tert*-butoxycarbonyl)-homocysteinate (2).** This compound was synthesized as described for **7** above, from **6** (200 mg, 0.68 mmol) and 1,3-dibromopropane (420 mg, 2.06 mmol). The crude residue was purified by chromatography on silica gel (heptanes/ethyl acetate 90:10) to give **2** (215 mg, 77%) as a yellow oil. HPLC purity, 99%. ^{1}H NMR ($CDCl_3$, 400 MHz): δ 5.15−5.05 (m, 1H), 4.35−4.20 (m, 1H), 3.51 (t, J = 6.7 Hz, 2H), 2.67 (t, J = 6.7 Hz, 2H), 2.60−2.50 (m, 2H), 2.15−2.05 (m, 1H), 2.10−2.05 (qu, J = 6.7 Hz, 2H), 1.95−1.80 (m, 1H), 1.47 (s, 9H), 1.44 (s, 9H). ^{13}C NMR ($CDCl_3$, 100 MHz): δ 171.43, 155.47, 82.37, 79.98, 53.53, 33.34, 32.31, 32.21, 30.36, 28.47, 28.16, 28.02. LRMS: ES(+ve) m/z 412 (M[^{79}Br] + 1), 414 (M[^{81}Br] + 1). HRMS: ES(+ve) calcd for $C_{15}H_{28}NO_4SBr$ (M[^{79}Br]), 412.1157; found, 412.1165.

***tert*-Butyl *N*-(*tert*-butoxycarbonyl)-*S*-(3-chloropropyl)-homocysteinate (3).** This compound was synthesized as described for **7** above, from **6** (200 mg, 0.68 mmol) and 1-bromo-3-chloroethane (327 mg, 2.06 mmol). The crude residue was purified by chromatography on silica gel (heptanes/ethyl acetate 90:10) to give **3** (236 mg, 94%) as a yellow oil. HPLC purity, 99%. ^{1}H NMR ($CDCl_3$, 400 MHz): δ 5.15−5.05 (m, 1H), 4.35−4.20 (m, 1H), 3.64 (t, J = 6.7 Hz, 2H), 2.67 (t, J = 6.7 Hz, 2H), 2.60−2.50 (m, 2H), 2.15−2.05 (m, 1H), 2.02 (qu, J = 6.7 Hz, 2H), 1.95−1.80 (m, 1H), 1.47 (s, 9H), 1.44 (s, 9H). ^{13}C NMR ($CDCl_3$, 100 MHz): δ 171.43, 155.48, 82.36, 79.97, 53.53, 43.54, 33.32, 32.25, 29.16, 28.46, 28.16, 28.03. LRMS: ES(+ve) m/z 368 (M[^{35}Cl] + 1), 370 (M[^{37}Cl] + 1). HRMS: ES(+ve) calcd for $C_{16}H_{30}NO_4SCl$ (M[^{35}Cl] + 1), 368.1662; found, 368.1677.

***tert*-Butyl *N*-(*tert*-butoxycarbonyl)-*S*-(3-tosyloxypropyl)-homocysteinate (1).** To a solution of **8** (2.85 g, 8.20 mmol) in acetonitrile (115 mL) was added *N*,*N*,*N*′,*N*′-tetramethyl-1,6-hexanediamine, (2.84 g, 16.14 mmol) followed by *p*-toluenesulfonyl chloride (2.39 g, 12.30 mmol), and the reaction mixture was stirred for 4 h at room temperature under nitrogen. The reaction mixture was diluted with water (340 mL) and extracted with ethyl acetate (3 × 340 mL). The combined organic layers were washed with brine (340 mL) and dried ($MgSO_4$), and the solvents evaporated. The crude residue was purified by chromatography on silica gel (heptanes/ethyl acetate 80:20) to give **1** (3.19 g, 77%) as a yellow oil. HPLC purity, 99%. ^{1}H NMR ($CDCl_3$, 400 MHz): δ 7.78 (d, J = 8.2 Hz, 2H), 7.34 (d, J = 8.2 Hz, 2H), 5.15−5.05 (m, 1H), 4.30−4.15 (m, 1H), 4.12 (t, J = 6.7 Hz, 2H), 2.53 (t, J = 6.7 Hz, 2H), 2.50−2.40 (m, 2H), 2.45 (s, 3H), 2.10−1.95 (m, 1H), 1.90 (qu, J = 6.7 Hz, 2H), 1.90−1.75 (m, 2H), 1.46 (s, 9H), 1.43 (s, 9H). ^{13}C NMR ($CDCl_3$, 100 MHz): δ 171.37, 155.47, 144.97, 133.15, 130.03, 128.05, 82.37, 79.97, 68.88, 53.51, 33.19, 29.82, 28.45, 28.14, 27.99, 27.97, 21.78. LRMS: ES(+ve) m/z 526 (M + Na). HRMS: ES(+ve) calcd for $C_{23}H_{37}NO_7S_2$ (M + 1), 504.2090; found, 504.2105.

***S*-(3-Fluoropropyl)homocysteine Hydrochloride (FPH-Cys).** To a solution of the protected amino acid **7** (63 mg) in THF (530 μL) was added 6 N hydrochloric acid (1.07 mL), and the reaction mixture was stirred at room temperature for 3 h. The solvent was removed under reduced pressure, and the resulting solid was washed with ethyl acetate (3 × 7 mL) and dried under vacuum to give FPHCys (38 mg, 91%) as a white solid; mp 107−109 °C. HPLC purity, 98%. ^{1}H NMR (D_2O, 400 MHz): δ 4.64 (dt, J = 47.1 Hz, J = 5.8 Hz, 2H), 4.17 (t, J = 6.2 Hz, 1H), 2.77 (t, J = 7.3 Hz, 2H), 2.75 (t, J = 7.0 Hz, 2H), 2.35−2.15 (m, 2H), 2.10−1.95 (m, 2H). ^{13}C NMR (D_2O, 100 MHz): δ 173.52, 84.88 (d, J = 158.7 Hz), 53.52, 30.81, 30.69 (d, J = 19.9 Hz), 27.84 (d, J = 5.4 Hz), 27.64. LRMS: ES(+ve) m/z 196 (M + 1). HRMS: ES(+ve) calcd for $C_7H_{14}NO_2SF$ (M + 1), 196.0808; found, 196.0814.

Radiosynthesis of [^{18}F]FPHCys. The radiolabeling of [^{18}F]-L-FPHCys and [^{18}F]-D-FPHCys was performed on a GE Tracerlab FX_{FN} synthesis module using an in-house reaction sequence. On the GE Tracerlab FX_{FN} synthesis module, aqueous [^{18}F]fluoride solution (18−37 GBq) was loaded on a QMA cartridge first activated with potassium carbonate (10 mL, 0.10 M). The concentrated [^{18}F]fluoride was eluted into the reactor with 1 mL of a solution of $K_2C_2O_4/K_2CO_3$ (2.55 mg/50 μg) and $K_{2.2.2.}$ (10 mg) in a 1:4 ratio of acetonitrile/water. The solvent was evaporated under vacuum and a stream of helium at 70 °C for 7 min and then at 120 °C under vacuum only for 5 min. To the activated $K_{2.2.2.}$/potassium [^{18}F]fluoride was added the tosylate precursor **1** (5 mg, 10 μmol) in acetonitrile (2 mL), and the mixture was heated at 100 °C for 10 min. The reactor was cooled to 30 °C, and 6 N HCl (500 μL) was added. After 3 min at 100 °C, the acetonitrile was evaporated under a stream of helium at 100 °C for 2 min. The reactor was then cooled to 30 °C and sequentially treated with 6 N NaOH (500 μL) and phosphate buffer, pH 6 (1 mL, 1.5 M). This solution was directly passed through a Sep-Pak Light Alumina N before purification on a preparative reverse phase HPLC column (Atlantis C18 T3 column (250 mm × 10 mm, 5 μm); mobile phase ethanol/phosphate buffer, pH 6, 0.15 M (5:95, v/v); flow rate, 3 mL/min; λ = 220 nm). The fraction containing the labeled product [^{18}F]FPHCys was collected between 15 and 16 min, passed through a 0.22 μm filter, and recovered in a sterile vial for dilution with sodium chloride. Routinely, [^{18}F]FPHCys was ready for injection

in approximately 65 min. Typically, 4.1−7.8 GBq of [^{18}F]-L-FPHCys or [^{18}F]-D-FPHCys was isolated in 20 ± 5% nondecay-corrected.

The chemical and radiochemical purity of [^{18}F]-L-FPHCys and [^{18}F]-D-FPHCys were analyzed on a Phenomenex Gemini column (150 mm × 4.6 mm, 5 μm) with a flow of 1 mL/min and phosphate buffer, pH 11.5, 0.05 M, as the mobile phase. The retention time was between 13.5 and 14.5 min for [^{18}F]-L-FPHCys and [^{18}F]-D-FPHCys, and the identity of the labeled compound was confirmed by coinjection with the authentic [^{19}F]FPHCys standard on HPLC. Typically, both enantiomers of [^{18}F]FPHCys were synthesized with a radiochemical purity >98% and a specific activity >185 GBq/μmol starting from 18 to 37 GBq of [^{18}F]fluoride.

The enatiomeric purity of [^{18}F]-L-FPHCys and [^{18}F]-D-FPHCys was analyzed using chiral HPLC analysis, using a Phenomenex Chirex D Penicillamine column (150 mm × 4.6 mm, 5 μm) with a flow of 1 mL/min and isopropanol/$CuSO_{4aq}$, 2 nM (1:9, v/v), as the mobile phase. The retention time was 10.5−11.5 min for [^{18}F]-L-FPHCys and 13−14 min for [^{18}F]-D-FPHCys. The identity of each enantiomer was confirmed by coinjection with the L-FPHCys and D-FPHCys standard on HPLC. Typically, [^{18}F]-L-FPHCys and [^{18}F]-D-FPHCys were synthesized with an enantiomeric purity greater of >98%.

Cell Cultures. A375 human amelanotic melanoma cells and HT29 human colon adenocarcinoma cells lines were cultured in RPMI-1640 medium supplemented with 10% fetal bovine serum and 2 mM L-glutamine. Cells were maintained in 175 cm^2 flasks in a 5% CO_2, 37 °C humidified incubator.

Cell Uptake Studies. In 24-well culture plates, 2.5 × 10^5 cells were seeded in complete medium and left to attach overnight. The following day, the number of cells per well were counted in triplicate for each cell line. Before incubation with the radiotracer, the growth media were removed, and the cells were washed once with warm PBS to remove all traces of growth media. [^{18}F]-L-FPHCys and [^{18}F]-D-FPHCys were formulated in warm PBS. Freshly prepared radiotracer (0.37 MBq in 500 μL) was added, and the cells were incubated at 37 °C for 2, 15, 30, 60, 120, 180, and 240 min. Uptake was terminated by removing the tracer solution and washing cells with ice-cold PBS. Subsequently, the cells were lysed with 500 μL of 0.2 N NaOH. Radioactivity in the cells was measured with a γ-counter. The results were expressed as percent of applied dose per 1 × 10^5 cells. All activities were corrected for decay.

Competitive Inhibition Studies in Cells. Inhibitor studies were carried out to investigate the transport mechanism involved in the uptake of [^{18}F]-FPHCys in tumor cells. BCH was used for system L, and *N*-methyl-α-aminoisobutyric acid (MeAIB) for system A. Cells were prepared as described for uptake studies. Cells were preincubated with 400 μL of inhibitor (12.5 mmol/L in PBS) or PBS (for controls) at 37 °C. Freshly prepared radiotracer (0.37 MBq in 100 μL) was added, and the cells were incubated at 37 °C for 30 min. Uptake was terminated as described for uptake studies. The percentage of uptake in the treatment groups relative to the control group was determined.

Biodistribution Studies in Tumor-Bearing Mice. Biodistribution studies were performed 26 days after tumor induction. The tissue distribution of radioactivity was determined in A375 tumor-bearing mice after intravenous injection of 0.8−1 MBq of [^{18}F]-L-FPHCys or [^{18}F]-D-FPHCys in 100 μL of saline. At 15, 30, 60, and 120 min postinjection of the radiotracer, groups of mice (n = 5) were sacrificed by CO_2 administration followed by cervical fracture and dissected. Selected organs were weighed, and the radioactivity was measured using a γ-counter. The percent injected dose (% ID) was calculated by comparison with suitable dilutions of the injected dose. Radioactivity concentrations were expressed as percent of injected dose per gram of wet tissue (% ID/g).

Metabolite Studies. The determination of unchanged radiotracer in the plasma, tumor, cortex, pancreas, and urine was performed by radio-HPLC analysis, at 0.25, 1, and 2 h after injection of 18−20 MBq of [^{18}F]-L-FPHCys or [^{18}F]-D-FPHCys. Plasma (50 μL) and urine (50 μL) were mixed with L-FPHCys or D-FPHCys (5 nmol in 5 μL of water) and KF (5 nmol in 5 μL of water) for direct injection onto the HPLC. Tissue samples (50 mg) in 500 μL of saline containing unlabeled FPHCys compound and KF were exposed for 2 min to an ultrasonic probe, and the mixture was centrifuged at 6000*g* for 5 min. The supernatant was collected and directly injected in HPLC. The radioactivity of the precipitate was measured to quantify the saline extraction efficiency.

Radio-HPLC analysis was performed using a reverse phase HPLC column (Atlantis C18 T3 column (150 mm × 4.6 mm, 5 μm); mobile phase methanol/phosphate buffer, pH 6, 0.15 M (5:95, v/v); flow rate, 1 mL/min; λ = 210 nm). The radioactivity peak corresponding to the authentic FPHCys was compared to the total activity registered in the radiochromatogram to give the fraction of unchanged ligand in the sample.

Incorporation of [^{18}F]-L-FPHCys and [^{18}F]-D-FPHCys into Proteins. To determine the extent of protein incorporation of the two different ^{18}F-labeled MET analogues, the protein-bound activity was determined by protein precipitation with TCA and SEC at 0.25, 1, and 2 h after injection of 18−20 MBq of [^{18}F]-L-FPHCys or [^{18}F]-D-FPHCys. Plasma (50 μL) and tissue samples (tumor, cortex, and pancreas) (50 mg) in 500 μL of 10% TCA containing unlabeled L-FPHCys or D-FPHCys (5 nmol in 5 μL of water) and KF (5 nmol in 5 μL of water) were exposed for 2 min to an ultrasonic probe, and the mixture was centrifuged at 6000*g* for 5 min. The supernatant was collected, and this process was repeated twice on the remaining precipitate with 250 μL of 10% TCA. The radioactivity of the precipitate and supernatant was measured to quantify the incorporation of [^{18}F]FPHCys into proteins, in the sample.

Additionally, plasma (50 μL) was mixed with L-FPHCys or D-FPHCys (5 nmol) and KF (5 nmol) for direct injection onto SEC. Tissue samples (50 mg) in 500 μL of saline containing unlabeled FPHCys compound and KF were exposed for 2 min to an ultrasonic probe, and the mixture was centrifuged at 6000*g* for 5 min. The supernatant was collected and directly injected onto SEC. The radioactivity of the precipitate was measured to quantify the saline extraction efficiency. SEC analysis was performed using a size exclusion column (Phenomenex BioSep SEC S2000 column (300 mm × 7.8 mm); mobile phase phosphate buffer, pH 7, 50 mM; flow rate, 1 mL/min; λ = 210 and 254 nm). The radioactivity peak corresponding to the authentic FPHCys was compared to the total activity registered in the radiochromatogram to give the fraction of quantify the incorporation of [^{18}F]FPHCys into proteins, in the sample.

PET Imaging Studies in Tumor-Bearing Mice. The mouse was anaesthetized via inhalant isoflurane in 200 mL/min oxygen during the imaging study. A 10 min CT scan was performed on each subject for anatomical information, followed by a 2 h PET scan. The mouse was injected intravenously with 18−20 MBq of [^{18}F]-L-FPHCys or [^{18}F]-D-FPHCys in 100 μL of saline. Image acquisition commenced simultaneously with radiotracer injection. The data were histogrammed into 25 consecutive frames and reconstructed with an iterative algorithm (3D OSEM/FastMap). PET and CT volumes are automatically coregistered and visualized with Brainvisa (http://brainvisa.info).

■ ASSOCIATED CONTENT

Supporting Information. Reactivity of precursor **1**−**3** using potassium carbonate or potassium oxalate for the radiolabeling, HPLC profile of [^{18}F]FPHCys for the radiosynthesis and QC analysis, and reaction sequence and preparation of reagent for the [^{18}F]FPHCys radiosynthesis. This material is available free of charge via the Internet at http://pubs.acs.org.

AUTHOR INFORMATION

Corresponding Author
*Tel: +61 2 9717 3292. Fax: +61 2 9717 9262. E-mail: bts@ansto.gov.au.

ACKNOWLEDGMENT

We thank Allira Schuster-Woodhouse, Cathy D. Jiang, Dr. Tien Pham, and Naomi Wyatt for their assistance with radiolabeling development and metabolite studies and Drs. Oliver Neels and Peter Roselt for their support in translating and validating the synthetic process at the Peter MacCallum Cancer Centre for ongoing characterization studies. This study was funded by the Cooperative Research Centre for Biomedical Imaging Development Ltd (CRC-BID), Bundoora, Victoria, Australia, established and supported under the Australian Government's Cooperative Research Centres program.

ABBREVIATIONS USED

BCH, 2-amino-bicyclo[2.2.1]heptane-2-carboxylic acid; DMF, dimethylformamide; HPLC, high-pressure liquid chromatography; ID, injected dose; $K_{2.2.2.}$, 4,7,13,21,24-hexaoxa-1,10-diazabicyco[8.8.8]hexacosane; OSEM, ordered subset expectation maximization; PET, positron emission tomography; SEC, size exclusion chromatography; TCA, trichloroacetic acid

REFERENCES

(1) Shreve, P. D.; Anzai, Y.; Wabl, R. L. Pitfalls in oncologic diagnosis with FDG PET imaging: Physiologic and benign variant. *Radiographics* **1999**, *19*, 61–77.

(2) Johnstone, R. M.; Sholefield, P. G. Amino acid transport in tumour cells. *Adv. Cancer Res.* **1965**, *9*, 143–226.

(3) Jager, P. L.; Vaalburg, W.; Prium, J.; De Vries, E. G. E.; Langen, K. J.; Piers, D. A. Radiolabeled amino acids: Basic aspects and clinical applications in oncology. *J. Nucl. Med.* **2001**, *42*, 432–435.

(4) Langen, K. L.; Ziemons, K.; Kiwit, J. C. W.; Herzog, H.; Kuwert, T.; Bock, W. J.; Stöcklin, G.; Feinendegen, L. E.; Müller-Gartner, H. W. 3-[^{123}I]Iodo-α-methyltyrosine and [methyl-^{11}C]-L-methionine uptake in cerebral gliomas: A comparative study using SPECT and PET. *J. Nucl. Med.* **1997**, *38*, 517–522.

(5) Becherer, A.; Karanikas, G.; Szabo, M.; Zettinig, G.; Asenbaum, S.; Marosi, C.; Henk, C.; Wunderbaldinger, P.; Czech, T.; Wadsak, W.; Kletter, K. Brain tumour imaging with PET: A comparison between [^{18}F]fluorodopa and [^{11}C]methionine. *Eur. J. Nucl. Med. Mol. Imaging* **2003**, *30*, 1561–1567.

(6) Weber, W. A.; Wester, H. J.; Grosu, A. L.; Herz, M.; Dzewas, B.; Fedlmann, H. J.; Molls, M.; Stöcklin, G.; Schwaiger, M. O-(2-[^{18}F]Fluoroethyl)-L-tyrosine and L-[methyl-^{11}C]methionine uptake in brain tumours: Initial results of a comparative study. *Eur. J. Nucl. Med.* **2000**, *27*, 542–549.

(7) Leskinene-Kallio, S.; Ruotsalainen, U.; Någren, K.; Teräs, M.; Joensuu, H. Uptake of carbon-11-methionine and fluorodeoxyglucose in non-Hodgkin's lymphoma: A PET study. *J. Nucl. Med.* **1991**, *32*, 1211–1218.

(8) Nettelbladt, O. S.; Sundin, A. E.; Valind, S. O.; Gustafsson, G. R.; Lamberg, K.; Långstrom, B.; Björnsson, E. H. Combined fluorine-18-FDG and carbon-11-methionine PET for diagnosis of tumors in lung and mediastinum. *J. Nucl. Med.* **1998**, *39*, 640–647.

(9) Leskinene-Kallio, S.; Någren, K.; Lehikoinen, P.; Ruotsalainen, U.; Joensuu, H. Uptake of ^{11}C-methionine in breast cancer studied by PET. An association with the size of S-phase fraction. *Br. J. Cancer* **1991**, *64*, 1121–1124.

(10) Vaalburg, W.; Coenen, H. H.; Crouzel, C.; Elsinga, PH. H.; Långstrom, B.; Lemaire, C.; Meyer, G. J. Amino acids for the measurement of protein syntheis In Vivo by PET. *Nucl. Med. Biol.* **1992**, *19*, 227–237.

(11) Laverman, P.; Boerman, O. C.; Corstens, F. H. M.; Oyen, W. J. G. Fluorinated amino acids for tumour imaging with positron emission tomography. *Eur. J. Nucl. Med.* **2002**, *29*, 681–690.

(12) Coenen, H. H.; Kling, P.; Stöcklin, G. Cerebral metabolism of L-[2-^{18}F]fluorotyrosine, a new PET tracer of protein synthesis. *J. Nucl. Med.* **1989**, *30*, 1367–1372.

(13) Langen, K.-J.; Jarosch, M.; Mühlensiepen, H.; Hamacher, K.; Bröer, S.; Jansen, P.; Zilles, K.; Coenen, H. H. Comparison of fluorotyrosines and methionine uptake in F98 rat gliomas. *Nucl. Med. Biol.* **2003**, *30*, 501–508.

(14) Wienhard, K.; Herholz, K.; Coenen, H. H.; Rudolf, J.; Kling, P.; Stöcklin, G.; Heiss, W. D. Increased amino acid transport in to brain tumors mesuared by PET of L-(2-^{18}F)fluorotyrosine. *J. Nucl. Med.* **1991**, *32*, 1338–1346.

(15) Kubota, K.; Ishiwata, K.; Kubota, R.; Yamada, S.; Takahashi, J.; Abe, Y.; Fukuda, H.; Ido, T. Feasibility of Fluorine-18-Fluorophenylalanine for Tumor Imaging Compared with Carbon-11-L-Methionine. *J. Nucl. Med.* **1996**, *37*, 320–325.

(16) Ishiwata, K.; Kubota, K.; Murakami, M.; Kubota, R.; Sasaki, T; Ishii, S.; Senda, M. Re-evaluation of amino acid PET studies: Can the protein synthesis rates in brian and tumour tissues be measured In Vivo. *J. Nucl. Med.* **1993**, *34*, 1936–1943.

(17) Inoue, T.; Tomiyoshi, K.; Higuichi, T.; Ahmed, K.; Sarwar, M.; Aoyagi, K.; Amano, S.; Alyafei, S.; Zhang, H.; Endo, K. Biodistribution studies on L-3-[fluorine-18]fluoro-α-methyl tyrosine: A potential tumor-detecting agent. *J. Nucl. Med.* **1998**, *39*, 663–667.

(18) Inoue, T.; Shibasaki, T.; Oriuchi, N.; Aoyagi, K.; Tomiyoshi, K.; Amano, S.; Mikuni, M.; Ida, I.; Aoki, J.; Endo, K. ^{18}F α-Methyl tyrosine PET studies in patients with brain tumors. *J. Nucl. Med.* **1999**, *40*, 399–405.

(19) Wester, H. J.; Herz, M.; Weber, W.; Heiss, P.; Senekowitsch-Schmidtke, R.; Schwaiger, M.; Stöcklin, G. Synthesis and radiopharmacology of *O*-(2-[^{18}F]Fluoroethyl)-L-tyrosine for tumor imaging. *J. Nucl. Med.* **1999**, *40*, 205–212.

(20) Pauleit, D; Stoffels, G.; Bachofner, A.; Floeth, F. W.; Sabel, M.; Herzog, H.; Tellmann, L.; Jansen, P.; Reifenberger, G.; Hamacher, K.; Coenen, H. H.; Langen, K. J. Comparison of ^{18}F-FET and ^{18}F-FDG PET in brain tumors. *Nucl. Med. Biol.* **2009**, *36*, 779–787.

(21) Heiss, P.; Mayer, S.; Herz, M.; Wester, H. J.; Schwaiger, M.; Senekowitsch-Schmidtke, R. Investigation of transport mechanism and uptake kinetics of *O*-(2-[^{18}F]Fluoroethyl)-L-tyrosine in vitro and In Vivo. *J. Nucl. Med.* **1999**, *40*, 1367–1373.

(22) McConathy, J.; Martarello, L.; Malveaux, E. J.; Camp, V. M.; Simpson, N. E.; Simpson, C. P.; Bowers, G. D.; Zhang, Z.; Olson, J. J.; Goodman, M. M. Synthesis and evaluation of 2-amino-4-[^{18}F]fluoro-2-methylbutanoic acid (FAMB): Relationship of amino acid transport to tumor imaging properties of branched fluorinated amino acids. *Nucl. Med. Biol.* **2003**, *30*, 477–490.

(23) McConathy, J.; Martarello, L.; Malveaux, E. J.; Camp, V. M.; Simpson, N. E.; Simpson, C. P.; Bowers, G. D.; Olson, J. J.; Goodman, M. M. Radiolabeled amino acids for tumor imaging with PET: Radiosynthesis and biological evaluation of 2-amino-3-[^{18}F]fluoro-2-methylpropanoic acid and 3-[^{18}F]fluoro-2-methyl-2-(methylamino)propanoic acid. *J. Med. Chem.* **2002**, *45*, 2240–2249.

(24) Shoup, T. M.; Goodman, M. M. Synthesis of [^{18}F]-1-amino-3-fluorocyclobutane-1-carboxylic acid (FACBC): A PET tracer for tumor delineation. *J. Labelled Compd. Radiopharm.* **1999**, *42*, 215–225.

(25) Shoup, T. M.; Olson, J.; Hoffman, J. M.; Votaw, J.; Eshima, D.; Eshima, L.; Camp, V. M.; Stabin, M.; Votaw, D.; Goodman, M. M. Synthesis and evaluation of [^{18}F]1-amino-3-fluorocyclobutane-1-carboxylic acid to image brain tumors. *J. Nucl. Med.* **1999**, *40*, 331–338.

(26) McConathy, J.; Voll, R. J.; Yu, W.; Crowe, R. J.; Goodman, M. M. Improved synthesis of anti-[^{18}F]FACBC: Improved preparation of labelling precursor and automated radiosynthesis. *Appl. Radiat. Isot.* **2003**, *58*, 657–666.

(27) Martarello, L.; McConathy, J.; Camp, V. M.; Malveaux, E. J.; Simpson, N. E.; Simpson, C. P.; Olson, J. J.; Bowers, G. D.; Goodman, M. M. Synthesis of syn and anti-1-amino-3-[^{18}F]fluoromethyl-cyclobutane-1-carboxylic acid (FMACBC), potential PET ligands for tumor detection. *J. Med. Chem.* **2002**, *45*, 2250–2259.

(28) Stryer, L. Biosynthesis of amino acids and heme. *Biochemistry*; WH Freeman and Co.: New York, 1995; pp 713−738.

(29) Stryer, L. Amino acid degradation and the urea cycle. *Biochemistry*; WH Freeman and Co.: New York, 1995; pp 629−652.

(30) Bourdier, T.; Fookes, C. J. R.; Pham, T. Q.; Greguric, I.; Katsifis, A. Synthesis and stability of *S*-(2-[^{18}F]fluoroethyl)-L-homocysteine for potential tumour imaging. *J. Labelled Compd. Radiopharm.* **2008**, *51*, 369–373.

(31) Tang, G.; Wang, M.; Tang, X.; Luo, L.; Gan, M. Fully automated synthesis module for preparation of *S*-(2-[^{18}F]fluoroethyl)-L-methionine by direct nucleophilic exchange on a quaternary 4-amino-pyridinium resin. *Nucl. Med. Biol.* **2003**, *30*, 509–512.

(32) Serafinowski, P.; Dorland, E.; Harrap, K. R.; Balzarini, J.; De Clercq, E. Synthesis and antiviral activity of some new *S*-adenosyl-L-homocysteine derivatives. *J. Med. Chem.* **1992**, *35*, 4576–4583.

(33) Zhu, J.; Hu, X.; Dizin, E.; Pei, D. Catalitic mechanism of *S*-ribosylhomocysteinase (LuxS): Direct observation of ketone intermediates by ^{13}C NMR spectroscopy. *J. Am. Chem. Soc.* **2003**, *125*, 13379–13381.

(34) Yoshiizumi, K.; Nakajima, F.; Dobashi, R.; Nishimura, N.; Ikeda, S. Studies on scavenger receptor inhibitors. Part 1: Synthesis and structure-activity relationships of novel derivatives of sulfatides. *Bioorg. Med. Chem.* **2002**, *10*, 2445–2460.

(35) Lherbet, C.; Keillor, J. W. Probing the stereochemistry of the active site of gamma-glutamyl transpeptidase using sulfur derivatives of L-glutamic acid. *Org. Biomol. Chem.* **2004**, *2*, 238–245.

(36) Yoshida, Y.; Shimonishi, K.; Sakakura, Y.; Okada, S.; Aso, N.; Tanabe, Y. Facile and practical methods for the sulfonylation of alcohols using Ts(Ms)Cl and $Me_2N(CH_2)_nNMe_2$ as a key base. *Synthesis* **1999**, *9*, 1633–1636.

(37) Hamacher, K.; Coenen, H. H. Efficient routine production of the ^{18}F-labelled amino acid *O*-(2-[^{18}F]Fluoroethyl)-L-tyrosine. *Appl. Radiat. Isot.* **2002**, *57*, 853–856.

(38) Hamacher, K. Protected tyrosine derivates, method for the production thereof and use of the same for producing *O*-(2-[^{18}F]-fluoroethyl)-L-tyrosine. U.S. Patent 6,919,475, 2005.

(39) Schober, O.; Duden, C.; Meyer, G. J.; Muller, J. A.; Hundeshagen, H. Non selective transport of [^{11}C-methyl]-L- and D-methionine into a malignant glioma. *Eur. J. Nucl. Med.* **1987**, *13*, 103–105.

(40) Yanagida, O.; Kanai, Y.; Chairoungdua, A.; Kim, D. K.; Segawa, H.; Nii, T.; Cha, S. H.; Matsuo, H.; Fukushima, J.; Fukasawa, Y.; Tani, Y.; Taketani, Y.; Uchino, H.; Kim, J. Y.; Inatomi, J.; Okayasu, I.; Miyamoto, K.; Takeda, E.; Goya, T.; Endou, H. Human L-type amino acid transporter 1 (LAT1): Characterization of function and expression in tumor cell lines. *Biochim. Biophys. Acta* **2001**, *1514*, 291–302.

(41) Segawa, H.; Fukasawa, Y.; Miyamoto, K. I.; Takeda, E.; Endou, H.; Kanai, Y. Identification and fuctional characterization of a Na^+-independent neural amino acid transporter with broad substrate selectivity. *J. Biol. Chem.* **1999**, *274*, 19745–19751.

(42) Wester, H. J.; Herz, M.; Weber, W.; Senekowitsch-Schmidtke, R.; Schwaiger, M.; Stöcklin, G.; Hamacher, K. Preclinical evaluation of 4-[^{18}F]fluoroprolines: Diastereomeric effect on metabolism and uptake in mice. *Nucl. Med. Biol.* **1999**, *26*, 259–265.

(43) Tsukada, H.; Sato, K.; Fukumoto, D.; Kakiuchi, T. Evaluation of D-isomers *O*-^{18}F-fluoromethyl, *O*-^{18}F-fluoroethyl and *O*-^{18}F-fluoropropyl tyrosine as tumor imaging agents in mice. *Eur. J. Nucl. Med. Mol. Imaging* **2006**, *33*, 1017–1024.

(44) Tsukada, H; Sato, K.; Fukumoto, D.; Nishiyama, S.; Harada, N.; Kakiuchi, T. Evaluation of D-isomers of *O*-^{11}C-methyl tyrosine and *O*-^{18}F-fluoromethyl tyrosine as tumor-imaging agents in tumor-bearing mice: Comparaison with L- and D-^{11}C-methionine. *J. Nucl. Med.* **2006**, *47*, 679–688.

(45) Ishiwata, K.; Kubota, K.; Murakami, M.; Kubota, R.; Senda, M. A comparative study on protein incorporation of L-[methyl-^{3}H]methiomine, L-[l-^{14}C]leucine and L-2-[^{18}F]fluorotyrosine in tumor bearing mice. *Nucl. Med. Biol.* **1993**, *20*, 895–899.

(46) Ishiwata, K.; Vaalburg, W.; Elsinga, P. H.; Paans, A. M. J.; Woldring, M. G. Metabolic studies with L-[l-^{14}C]tyrosine for the investigation of a kinetic model to measure protein synthesis rates with PET. *J. Nucl. Med.* **1988**, *29*, 524–529.

(47) Visser, E. P.; Disselhorst, J. A.; Brom, M.; Laverman, P.; Gotthardt, M.; Oyen, W. J. G.; Boerman, O. C. Spatial resolution and selectivity of the Inveon small-animal PET scanner. *J. Nucl. Med.* **2009**, *50*, 139–147.